Synthesis and Characterization of Temperature-Responsive Poly(vinyl alcohol)-Based Copolymers

Yuanfeng Pan,[1] Huining Xiao,[1,2] Guanglei Zhao,[1] Beihai He[1]

[1]*State Key Laboratory of Pulp and Paper Engineering, South China University of Technology, Guangzhou 510640, China*
[2]*Department of Chemical Engineering, University of New Brunswick, Fredericton, New Brunswick E3B 5A3, Canada*

Received 13 January 2008; accepted 5 April 2008
DOI 10.1002/app.28798
Published online 26 August 2008 in Wiley InterScience (www.interscience.wiley.com).

ABSTRACT: A poly(vinyl alcohol) (PVA)/sodium acrylate (AANa) copolymer was synthesized to improve the water solubility of PVA at the ambient temperature. Furthermore, a series of temperature-responsive acetalyzed poly (vinyl alcohol) (APVA)-*co*-AANa samples of various chain lengths, degrees of acetalysis (DAs), and comonomer contents were prepared via an acid-catalysis process. Fourier transform infrared and ^{1}H-NMR techniques were used to analyze the compositions of the copolymers. The measurement of the turbidity change for APVA-*co*-AANa aqueous solutions at different temperatures revealed that the lower critical solution temperature (LCST) of the copolymers could be tailored through the control of the molecular weight of the starting PVA-*co*-AANa, DA, and comonomer ratios. Lower LCSTs were observed for APVA-*co*-AANa with a longer chain length, a higher DA, and fewer acrylic acid segments. In addition, the LCSTs of the APVA-*co*-AANa aqueous solutions appeared to be salt-sensitive. The LCSTs decreased as the concentration of NaCl increased. Moreover, atomic force microscopy images of APVA-*co*-AANa around the LCST also proved the temperature sensitivity. © 2008 Wiley Periodicals, Inc. J Appl Polym Sci 110: 2698–2703, 2008

Key words: atomic force microscopy (AFM); copolymerization; functionalization of polymers; stimuli-sensitive polymers

INTRODUCTION

Stimulation-responsive polymers can perceive fine changes in external signals, such as the pH, temperature, electric field, or light, and produce corresponding changes or even mutations of the physical structure and chemical properties. Recently, much attention has been paid to research on stimulation-responsive polymers as intelligent materials. These polymers have a variety of applications, such as drug release, biosensors, biocatalysis, chemical memory, size selective separation, and energy transducers.[1] As stimulation-responsive polymers, thermally sensitive polymers exhibit sensitive responses in their structure, properties, and configuration to changes in the environmental temperature. Their aqueous solutions undergo fast, reversible changes around their lower critical solution temperature (LCST). Below the LCST, the free polymer chains are soluble in water and exist in an extended random coil conformation that is fully hydrated, mainly by hydrophobic hydration. On the contrary, above the LCST, the chains are hydrophobically folded and assemble to form a phase-separating state.[2]

Poly(*N*-isopropylacrylamide) (PNIPAM) is the most widely studied thermally sensitive polymer. In the past 30 years, there have been many publications describing the preparation, characterization, and applications of PNIPAM and related copolymers.[3–10] Although PNIPAM has some valuable properties that could be further applied to many fields, it is expensive and is suspected to be a carcinogen and neurotoxin, just like acrylamide.[11]

Poly(vinyl alcohol) (PVA) is a type of water-soluble polymer with cost effectiveness, innocuousness, and outstanding biological compatibility that has been widely applied in the field of biomedicine. Its aqua gel can be made into artificial cartilage, artificial brawn, wound compresses, and artificial crystals.[12–16] However, PVA does not possess thermal sensitivity or favorable water solubility. Moreover, PVA has poor mechanical properties because PVA films tend to contain massive bubbles. On the other hand, acrylic acid (AA) is a type of anionic polyelectrolyte that contains anionic groups and possesses excellent water solubility. The water solubility of PVA is improved if AA is incorporated into PVA chains. In this research, a PVA/sodium acrylate (AANa) copolymer was

Correspondence to: H. Xiao (hxiao@unb.ca).

Contract grant sponsor: National Natural Science Fund of Guangdong Province of China; contract grant number: 06Z002.
Contract grant sponsor: Fortieth Batch of the Chinese Postdoctoral Science Foundation; contract grant number: 20060400220.
Contract grant sponsor: Postdoctoral Innovation Foundation of South China University of Technology; contract grant number: 2006.

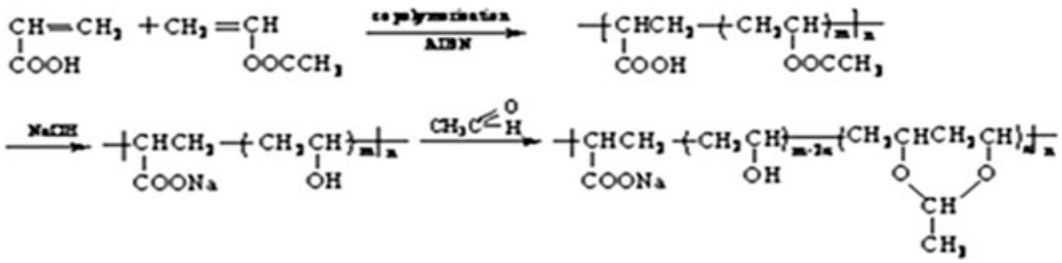

Figure 1 Synthesis of APVA-*co*-AANa.

synthesized first; the resulting copolymers were reacted with acetaldehyde in an acid solution to generate acetalyzed poly(vinyl alcohol) (APVA)-*co*-AANa polymer materials with temperature-responsive properties. The structure and LCST transition of APVA-*co*-AANa were studied through the manipulation of the molecular weight of the PVA-*co*-AANa matrix, the degree of acetalysis (DA), and the copolymer composition, and thus the structure–property relation was established for future architectural design of thermally sensitive polymer materials.

EXPERIMENTAL

Materials

Vinyl acetate (VAc) and AA were obtained from the Shanghai Puqiao Chemical Technology Graduate School (Shanghai, China) and purified via distillation before use. The initiator 2,2-azoisobutyronitrile was recrystallized twice with ethanol before use. Other chemicals were analytical-grade and were used without further purification.

Synthesis of PVA-*co*-AANa

The copolymerization of VAc with AA was carried out in a methanol solution. The predetermined amounts of VAc, AA, the initiator 2,2-azoisobutyronitrile, and methanol were placed in a three-necked flask under constant mechanical stirring. The solution was degassed and purged with N_2 and then was sealed and heated in a water bath at 60°C for 3 h. The viscous homogeneous solution was then dissolved in methanol, and a 2*N* NaOH methanol solution was added dropwise slowly at room temperature with stirring. When the phase transition occurred in the reaction system, a small amount of the NaOH methanol solution was dropped again. The reaction system was further stirred at room temperature for 1 h and then filtered, washed repeatedly with a methanol solution, and dried *in vacuo* at 50°C for 6 h.

Synthesis of APVA-*co*-AANa

A PVA-*co*-AANa solution was placed in a three-necked flask equipped with a mechanical stirrer, a dropping funnel, and a condenser. A chosen amount of HCl was added, and then acetaldehyde was added dropwise at 15°C for 30 min. After the completion of acetaldehyde feeding, the mixture was kept at 15°C for 1 h and at 28°C for 24 h. The reaction was stopped by neutralization with a 2*N* NaOH aqueous solution. The obtained solution was dialyzed for 24 h with a dialysis membrane with a molecular weight cutoff of 10,000. The synthesis is schematically shown in Figure 1.

Characterization techniques

IR spectra were recorded on a Nicolet (Madison, WI) Magna 550 Fourier transform infrared spectrophotometer. The NMR spectra were recorded in dimethyl sulfoxide-d_6 (DMSO-d_6) at 25°C with a Bruker (Fallanden, Switzerland) 400-MHz spectrometer operating at 300.13 and 75.5 MHz for ^{1}H and ^{13}C nuclei, respectively. The turbidity of APVA-*co*-AANa was determined with a Hach 2100AN turbidimeter (Loveland, CO). The molecular weight of PVA-*co*-AANa was determined with a Breeze 1515 gel permeation chromatograph (Milford, MA) using water as an eluent. Atomic force microscopy (AFM) images were obtained with a Nanoscope IIIa multimode scanning probe microscope with a J-scanner (maximum scan area = 125 × 125 μm^2; Veeco Instrument, Santa Barbara, CA).

Turbidity measurements

A Hach 2100AN turbidimeter was employed for the turbidity measurements. Samples were dissolved in deionized water or an NaCl solution at different concentrations and then placed into a water bath with temperature control. The samples were heated from 20°C in increments of 2.5°C. The samples were kept in the water bath for 10 min at each temperature and then were taken out and dried quickly before insertion into the turbidimeter. The turbidity was then recorded at each temperature.

AFM characterization

A Nanoscope IIIa multimode scanning probe microscope with a J-scanner (maximum scan area = 125 × 125 μm^2; Veeco Instrument) was operated in the

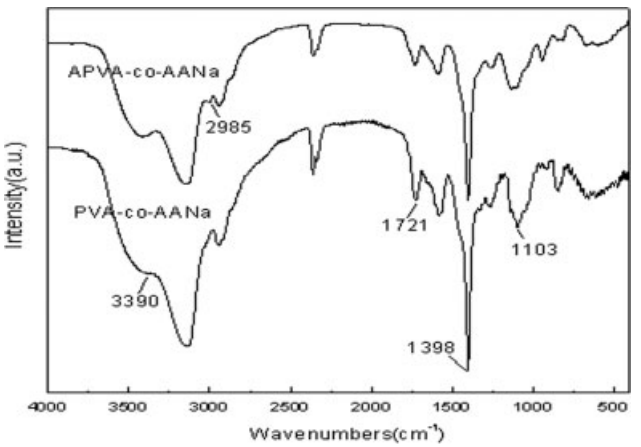

Figure 2 Fourier transform infrared spectra of PVA-*co*-AANa and APVA-*co*-AANa.

contact mode to record the images of the PVA-*co*-AANa and APVA-*co*-AANa films with a contact tip (NP-20 oxide-sharpened silicon nitride probes, Veeco NanoProbe, Santa Barbara, CA). The AFM images were flattened by the application of a first-order polynomial fit to remove defects from the image due to vertical (Z) scanner drift.

The sample preparation for AFM was conducted as follows: 0.1 mL of an APVA-*co*-AANa [weight-average molecular weight (M_w) = 67,459; VAc/AA = 95 : 5; DA = 30%; LCST = 43.0°C] solution at 0.044 wt % was deposited onto a freshly cleaned silicon wafer and then dried at 25 (below LCST) or 60°C (above LCST).

RESULTS AND DISCUSSION

Characterization of APVA-*co*-AANa

The IR spectra (Fig. 2) of PVA-*co*-AANa (M_w = 67,459) and APVA-*co*-AANa (DA = 30 mol %) show that the primary IR spectrum of PVA-*co*-AANa is similar to that of APVA-*co*-AANa, except for several weak characteristic absorptions. The bands at 1721 and 1103 cm^{-1} correspond to the C=O and C—O stretching vibrations of PVA-*co*-AANa. Strong bands at 3390 and 1398 cm^{-1} are the stretching vibration and transmutative vibration of —OH, which overlap with the characteristic absorption of poly(sodium acrylate) at 1400 cm^{-1}. In comparison with PVA-*co*-AANa, there is an antisymmetric stretching vibration of methyl C—H at 2985 cm^{-1} in the IR spectrum of APVA-*co*-AANa, thus confirming the reaction between PVA-*co*-AANa and acetaldehyde.

The IR spectra of PVA-*co*-AANa and APVA-*co*-AANa provide only limited structural information, whereas NMR techniques are extremely sensitive to the molecular composition.

^{1}H spectra of PVA-*co*-AANa and APVA-*co*-AANa are shown in Figure 3. The peaks for PVA-*co*-AANa are at 1.2–1.6 (CH_2) and 3.7–4.0 ppm (CH). The methylene proton resonances are rather broad because of a combination of spin–spin coupling and configurational splitting. Three distinct resonance signals of the hydroxyl proton appear at 4.65, 4.45, and 4.20 ppm, which are attributable to the syndiotactic, heterotactic, and isotactic triad sequences, respectively.[17,18] The peaks at 2.5 and 3.3 ppm are the resonance peaks of remnant protons from DMSO and water.

In comparison with those of the starting PVA-*co*-AANa, there are two new resonance peaks in the ^{1}H spectrum of APVA-*co*-AANa at 1.0–1.2 and 4.65 ppm, which are related to the acetal ring of APVA-*co*-AANa. The peaks at 1.0–1.2 ppm result from the methyl group of the acetal ring. The O—CH—O protons of the acetal ring appear at 4.65 ppm. They shifted to the lowest field because of the influence or coupling effect of the two adjacent oxygen atoms.

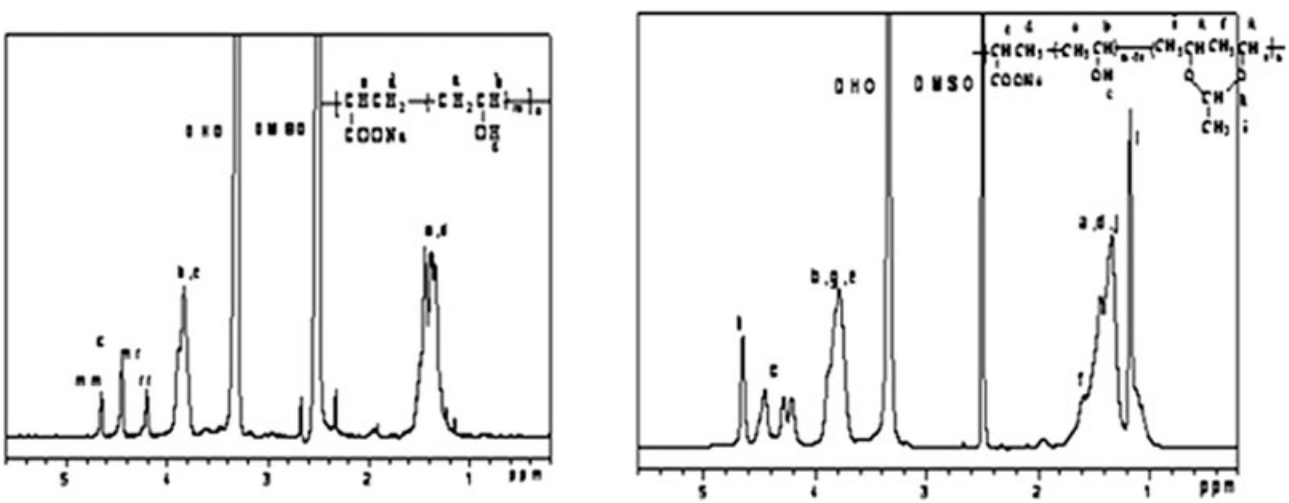

Figure 3 ^{1}H-NMR of (a) PVA-*co*-AANa and (b) APVA-*co*-AANa (M_w = 67,459).

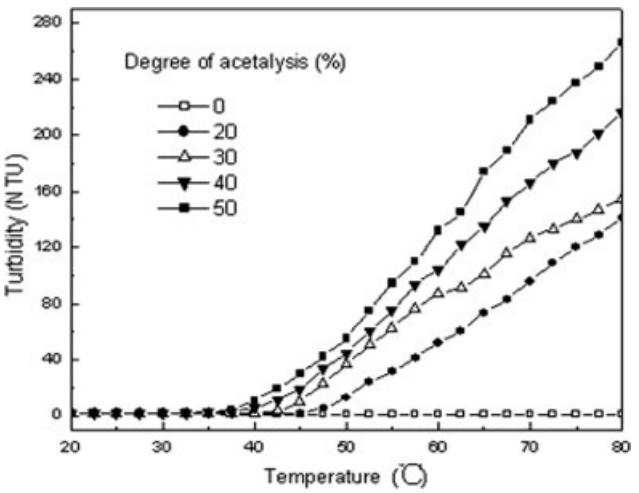

Figure 4 Turbidity of aqueous solutions containing PVA-*co*-AANa or APVA-*co*-AANa at different temperatures (10 mmol/L; VAc/AA = 95 : 5; M_w = 67,459).

These results further confirm that an acetylation reaction did occur between PVA-*co*-AANa and acetaldehyde.

Thermosensitivity of APVA-*co*-AANa

A series of APVA-*co*-AANa samples with different chain lengths, DAs, and comonomer ratios were prepared, and their phase-transition temperatures were investigated by turbidity. Turbidity curves were used to characterize the cloud point of an APVA aqueous solution. Turbidity is a measure of the clarity of water. The nephelometric turbidity unit was used as the turbidity unit in this research.

Influence of the DA on the LCST of APVA-*co*-AANa

The turbidity curves of aqueous solutions of APVA-*co*-AANa samples with different DAs (10 mmol/L; VAc/AA = 95 : 5; M_w = 67,459) at various temperatures are plotted in Figure 4. In our research, the cloud point or LCST is defined as the intersection of two straight lines drawn through the curves of turbidity at low and high temperatures, respectively. When the temperature was lower than the LCST, all three samples were transparent solutions, and their turbidities were close to 0; this indicated that the turbidity was independent of the temperature. However, after being heated to a certain temperature near the LCST, the transparent solutions of APVA-*co*-AANa started to become cloudy, and this was followed by a rapid increase in the turbidity. On the other hand, the PVA-*co*-AANa solution remained clear, and the turbidity was close to 0 during heating. The phase transition was the result of partial acetalization of the hydroxyl group on PVA-*co*-AANa. The acetal rings brought the hydrophobic group into the PVA-*co*-AANa chains. At low temperatures, the remaining hydroxyl groups on APVA-*co*-AANa formed intermolecular hydrogen bonds with water and/or cagelike structures surrounding the acetal rings to make APVA-*co*-AANa dissolve in water. Heating of the solution caused the destruction of the hydrogen bonds and exposure of the hydrophobic acetal rings, leading to the formation of hydrophobic aggregates or hydrophobic association, a phase-separated state. This corresponded to a morphological change from the random coils of APVA-*co*-AANa to intermolecular hydrophobic association.[19,20] Figure 4 shows that the LCSTs decreased continuously with increases in DA of APVA-*co*-AANa. The hydrophobic aggregates appeared at lower temperatures, so partial acetalization rendered APVA-*co*-AANa thermally sensitive. The phase-transition temperature of APVA-*co*-AANa could be readily tailored through the control of the DA.

Moreover, the acetal rings and carboxyl group of APVA-*co*-AANa chains facilitated the dissolution of PVA in cold water (e.g., 15°C). The APVA-*co*-AANa copolymer dissolved in water at room temperature much more readily than PVA, which had low solubility at the same temperature. With a very high degree of hydrolysis for PVA (98 mol % or greater), the copolymer formed strong interchain and intrachain hydrogen bonding, which made the polymer highly crystalline. For a highly hydrolyzed PVA, a preparation temperature greater than 80°C was required for complete dissolution in water in an acceptable time. We believe that, for this polymer, interchain and intrachain hydrogen bonding in the PVA chains is disrupted by thermal energy, thus increasing the solubility of PVA.

With APVA-*co*-AANa, the acetal rings disrupted interchain and intrachain hydrogen bonding and prevented APVA-*co*-AANa from forming crystals; that is, acetal rings and carboxyl groups increased the water solubility of APVA-*co*-AANa. Consequently, APVA-*co*-AANa could be dissolved in water at low temperatures and room temperature easily.

Effect of the copolymer molecular weight on the LCST of APVA-*co*-AANa

The LCST of APVA-*co*-AANa samples with the same DA but different molecular weights was studied in an attempt to explore the LCST transition rule of the copolymer. Table I lists the LCSTs of APVA-*co*-

TABLE I
LCST Values of APVA-*co*-AANa Samples of Different Molecular Weights

M_w	58,490	67,459	75,364	81,420
LCST (°C)	48.0	43.0	39.5	33.0

VAc/AA = 95 : 5; DA = 30%; 10 mmol/L.

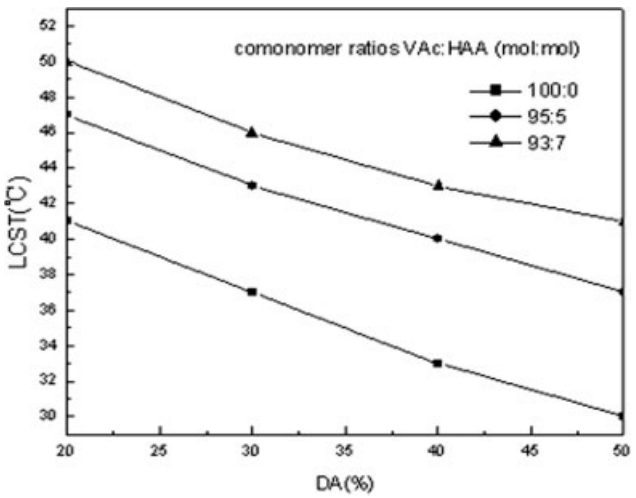

Figure 5 LCST values of APVA-*co*-AANa samples (10 mmol/L) with different monomer compositions and DAs.

AANa samples with different molecular weights at the same DA of 30%. At the same DA, the higher the molecular weight was of the starting PVA-*co*-AANa, the lower the phase-transition temperature was. This occurred because the longer the copolymer chains were, the higher the probabilities were of the backbone taking part in tangling and forming an association when the concentration of the solution reached a certain degree.

Influence of the comonomer ratios on the LCST of APVA-*co*-AANa

Figure 5 presents the LCSTs of APVA-*co*-AANa samples with different comonomer ratios and DA. At the same DA, the greater the AA component was of the starting PVA-*co*-AANa, the higher the phase-transition temperature was. This may have been due to the hydration force between $-COO^-$ and water, with the hydrogen bond getting stronger; this made the macromolecule disperse in water via loose and random coils at a higher temperature. Moreover, the greater the AA component was of the starting PVA-*co*-AANa, the better the solubility was at room temperature.

Effect of the electrolyte concentration on the LCST of APVA-*co*-AANa

To investigate the effect of cationic groups on the phase-transition temperature of APVA-*co*-AANa, NaCl or electrolyte solutions of various concentrations were used. The corresponding results for their transition temperatures are shown in Figure 6. Clearly, as the NaCl concentration increased, the LCST of APVA-*co*-AANa decreased linearly.

The reduction of the LCST of APVA-*co*-AANa is attributable to the existence of salt ions in the solution, which transformed the massive free water into hydrated water with salt ions. The hydrogen bonds between the polymers and hadrons were weakened, and the hydrated layers attached to the temperature-responsive macromolecules or chains were destroyed as well; this resulted in the increase of their hydrophobicity. The hydrophobicity of APVA-*co*-AANa increased as the LCST declined. Therefore, the ionic strength of the solution could have a direct impact on the hydrogen bonds.

AFM analysis of APVA-*co*-AANa

To visualize the changes in APVA-*co*-AANa chain conformation during the phase transition, AFM was used to image the actual physical states of polymer chains at a nanometer or subnanometer scale resolution as a function of temperature.

Figure 7(a,b) shows representative AFM images of APVA-*co*-AANa films formed at 25 and 60°C in air and observed in the contact mode. The AFM images reveal that the association or agglomeration of APVA-*co*-AANa chains occurred at 60°C. The APVA-*co*-AANa film that was dried at 60°C, above its LCST, had a flattened, globular appearance in the AFM image. On the other hand, the film that was dried at 20°C, below the LCST of APVA-*co*-AANa, had a smooth and uniform surface. This result suggests that the interaction between APVA-*co*-AANa chains and water is strong for the APVA-*co*-AANa molecule in its fully extended state at 25°C; that is, APVA-*co*-AANa is completely dissolved in water and forms a uniformly smooth film as the solvent is evaporated. At 60°C, the APVA-*co*-AANa chains collapse and tend to aggregate to form APVA-*co*-AANa chain globules. The nonacetalyzed PVA-*co*-AANa films were also prepared with the same procedure and dried at 25 or 60°C. The resulting AFM image (not presented herein) was similar to that shown in

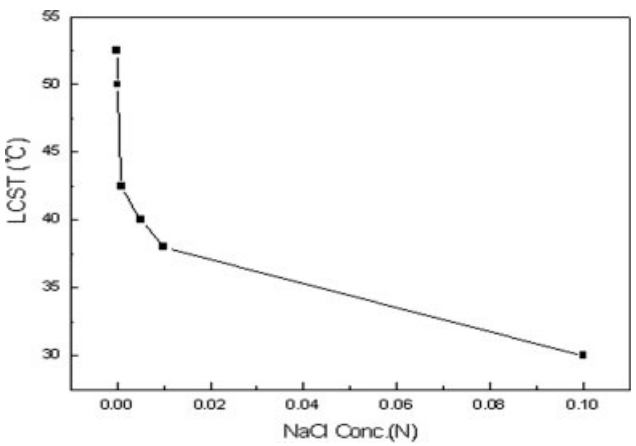

Figure 6 LCST values of APVA-*co*-AANa samples with different concentrations of NaCl (10 mmol/L; VAc/AA = 95 : 5; M_w = 67,459; DA = 30%).

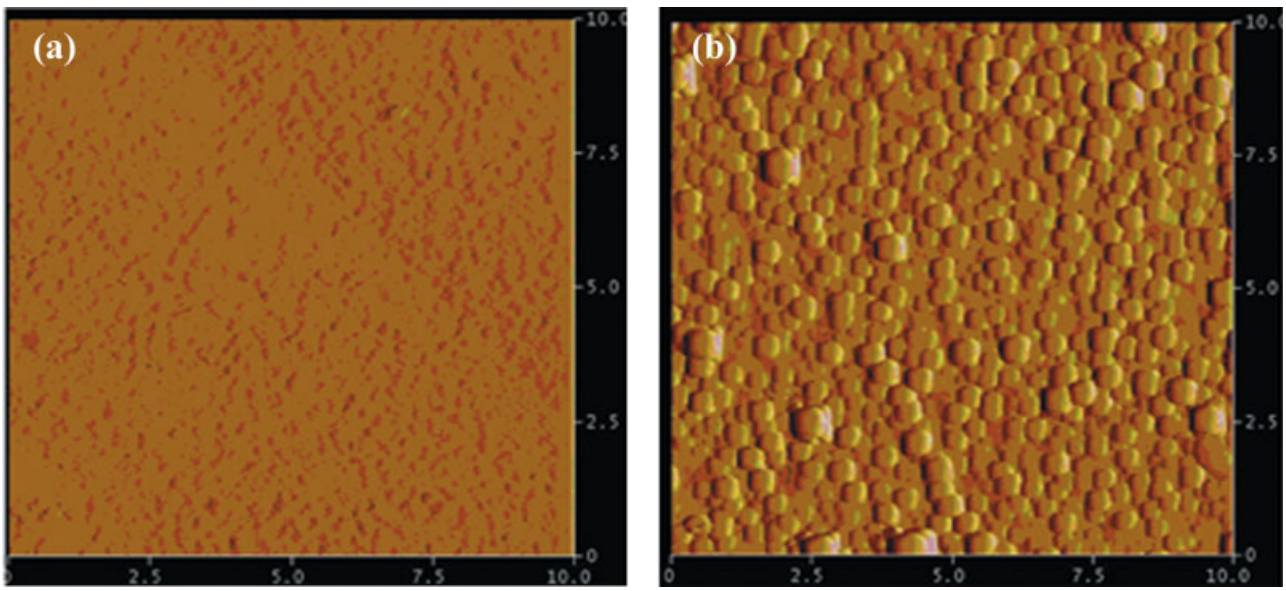

Figure 7 AFM images of APVA-*co*-AANa (10 mmol/L; VAc/AA = 95 : 5; M_w = 67,459; DA = 30%) at 25 and 60°C. [Color figure can be viewed in the online issue, which is available at www.interscience.wiley.com.]

Figure 7(a), or the films had smooth and uniform surfaces, regardless of the drying temperatures.

CONCLUSIONS

Hydrophobic acetal rings were introduced into APVA-*co*-AANa chains after a partial acetylation reaction, which rendered hydrophilic PVA-*co*-AANa partially hydrophobic or amphipathic. As a result, APVA-*co*-AANa became a temperature-responsive material. At low temperatures, water was a good solvent for APVA-*co*-AANa. As temperatures higher than the LCST, water became a poor solvent, so the polymer chains tended to aggregate or precipitate from the solution, and the solution turbidity increased accordingly. The LCST decreased continuously with an increases in DA of APVA-*co*-AANa. At the same DA, the higher the molecular weight was and the smaller the AA component was of the starting PVA-*co*-AANa, the lower the phase-transition temperature was. The LCST of APVA-*co*-AANa also decreased as the NaCl concentration in the solution increased. The phase transition was the result of partial acetalization of the hydroxyl group on PVA-*co*-AANa. The acetal rings generated by the reaction between acetaldehyde and hydroxyl of PVA-*co*-AANa brought hydrophobic groups into the PVA-*co*-AANa chains. At low temperatures, the remaining hydroxyl groups on APVA-*co*-AANa formed intermolecular hydrogen bonds with water and/or cage-like structures surrounding the acetal rings, allowing APVA-*co*-AANa to dissolve in water. AFM images visualized the morphological changes in APVA-*co*-AANa films dried at temperatures above the LCST or at 60°C.

References

1. Durme, K. V.; Rahier, H.; Mele, B. V. Macromolecules 2005, 38, 10155.
2. Scarpa, J. S.; Mueller, D. D.; Klotz, I. M. J Am Chem Soc 1967, 89, 6024.
3. Ono, Y.; Shikata, T. J Am Chem Soc 2006, 128, 10030.
4. Markus, N.; Katriina, K.; Antti, L.; Sami, H.; Heikki, T. J Polym Sci Part A: Polym Chem 2008, 46, 38.
5. Wu, K.; Shi, L. Q.; Zhang, W. Q.; An, Y. L.; Zhu, X. X. J Appl Polym Sci 2006, 102, 3144.
6. Chen, J. H.; Chen, H. H.; Chang, Y. X.; Chuang, P. Y.; Hong, P. D. J Appl Polym Sci 2008, 107, 2732.
7. Gotoh, T.; Okamoto, H.; Sakohara, S. Polym Bull 2007, 58, 213.
8. Choi, S. H.; Lee, J.; Choi, S. M.; Park, T. G. Langmuir 2006, 22, 1758.
9. Wang, X. L.; McCord, M. G. J Appl Polym Sci 2007, 104, 3614.
10. Zhai, G. Q. J Appl Polym Sci 2006, 100, 4089.
11. Pelton, R. Adv Colloid Interface Sci 2000, 85, 1.
12. Liu, Q. J Biomed Eng 2003, 20, 742.
13. Wu, L. G.; Zhang, Y. T.; Hu, S. H. J Donghua Univ 2001, 27, 114.
14. Yoshihiro, M.; Hitoshi, T.; Masanopi, Y. J Mater Sci 1997, 32, 491.
15. Arranz, F.; Sánchez-Chaves, M. Polym Bull 1995, 35, 533.
16. Kubo, M.; Hayakawa, N.; Minami, Y.; Tamura, M.; Uno, T.; Itoh, T. Polym Bull 2004, 52, 201.
17. Velden, G.; Beulen, J. Macromolecules 1982, 15, 1071.
18. Moritani, T.; Kuruma, I.; Shibatani, K.; Fujiwara, Y. Macromolecules 1972, 5, 577.
19. Li, L.; Shan, H.; Yue, C.; Lam, Y.; Tam, K. Langmuir 2002, 18, 7291.
20. Li, L. Macromolecules 2002, 35, 5990.